Available online at www.sciencedirect.com
SCIENCE DIRECT
Polymer 47 (2006) 2402–2410
polymer
www.elsevier.com/locate/polymer

Crystalline structures of intercalate molecular complexes of syndiotactic polystyrene with two fluorescent guests: 1,3,5-Trimethyl-benzene and 1,4-dimethyl-naphthalene

Oreste Tarallo [a], Vittorio Petraccone [a,*], Vincenzo Venditto [b], Gaetano Guerra [b]

[a] *Dipartimento di Chimica, Università di Napoli "Federico II", Complesso di Monte S. Angelo, Via Cintia, 80126 Napoli, Italy*
[b] *Dipartimento di Chimica, Università di Salerno, I-84081 Baronissi (SA), Italy*

Received 14 November 2005; received in revised form 9 January 2006; accepted 12 January 2006
Available online 24 February 2006

Abstract

The crystal structures of two molecular complex phases of syndiotactic polystyrene (s-PS) with 1,3,5-trimethyl-benzene (TMB) and 1,4-dimethyl-naphthalene (DMN) have been described. These structures present a monoclinic unit cell in which the s(2/1)2 polymer helices and guest molecules are packed according the space group $P2_1/a$ and unit cell constants: $a=17.3$ Å, $b=15.4$ Å, $c=7.8$ Å and $\gamma=95.7°$ for s-PS/TMB and $a=17.4$ Å, $b=17.2$ Å, $c=7.8$ Å and $\gamma=116.4°$ for s-PS/DMN. Both structures can be described as intercalates, since they present *ac* layers of polymer helices alternated to layers of contiguous guest molecules and a guest/monomeric-unit molar ratio of 1/2, as recently observed only for s-PS/norbornadiene molecular complex. On the basis of a comparison between crystalline structures and X-ray diffraction data of several s-PS molecular complexes, a simple criterion to anticipate their clathrate or intercalate nature has been suggested.

Keywords: Syndiotactic polystyrene; Intercalation compounds; Crystalline structure

1. Introduction

The complex polymorphic behavior of syndiotactic polystyrene (s-PS) has been extensively studied in the past years [1]. In particular, great attention has been reserved to the interesting property of this polymer to cocrystallize with a large variety of low molecular weight substances to form host–guest molecular complexes [1,2]. By removal of the guest molecules from any of these complexes, it is possible to obtain a nanoporous metastable polymorph of s-PS, the δ form, a host phase including centrosymmetric crystalline cavities (of nearly 120–160 $Å^3$ and cooperatively generated by two enantiomorphous polymer helices) in a molar ratio 1/4 with respect the styrene monomeric units [3]. Since this form is able to rapidly absorb selectively some organic substances from various environments (producing crystalline host–guest molecular complexes) its employment in the field of molecular sieves for the purification of water or gases [4], or as the sensing film of molecular sensors [5] has been proposed.

The self-assembling of the polymer host δ phase and several active guest molecules into crystalline molecular complexes can be relevant for several applications. In fact, polymer-based host–guest molecular complexes not only reduce the guest diffusivity and prevent guest self-aggregation (without recurring to chemical reactions), but also allow to control at molecular level the location and orientation of active guest molecules. In particular, the guest orientation control can be easily achieved by self-assembling with polymeric transparent films with axial [6] or uniplanar [7] orientations of their host crystalline phase. On this basis, films presenting s-PS/active-guest molecular complex phases have been proposed as advanced materials, mainly for optical applications (e.g. as fluorescent, photo-reactive and chromophore materials) [8]. This, of course, makes particularly relevant a precise definition of the crystal structure of s-PS molecular complexes, mainly for active guest molecules.

For most s-PS molecular complexes, isolated low-molecular-mass compounds are imprisoned as guest into the cavities of the nanoporous host δ phase, only producing minor changes to the packing of the polymer helices [2a–g,3]. These s-PS molecular complexes have been defined clathrate phases and are generally characterized by a guest/monomeric-unit molar ratio 1/4. Only for very small molecules, whose volume is much smaller than

* Corresponding author. Tel./fax: +39 081 674 309.
E-mail address: petraccone@chemistry.unina.it (V. Petraccone).

0032-3861/$ - see front matter © 2006 Elsevier Ltd. All rights reserved.
doi:10.1016/j.polymer.2006.01.056

the volume of the cavity of the host δ phase, more than one guest molecule can be hosted into each cavity. For instance, for I_2 [2d] and CS_2 [2f], two guest molecules are enclosed into each cavity and the guest/monomeric-unit molar ratio of these clathrate phases becomes 1/2.

Only recently and only for the molecular complex of s-PS with bicyclo[2,2,1]-hepta-2,5-diene (norbornadiene, NB), the occurrence of a different kind of s-PS molecular complex, defined as intercalate rather than clathrate, has been established [2h]. In fact, for the s-PS/NB molecular complex, the guest molecules are not isolated into host cavities but contiguous inside layers intercalated with mono-layers of enantiomorphous polymer helices. Of course, this intercalate structure presents a higher guest content with respect to the clathrate structures, in fact the guest/monomer-unit molar ratio is 1/2 rather than 1/4.

In this paper, we present the crystal structures of the molecular complexes of s-PS with two fluorescent molecules: 1,3,5-trimethyl-benzene (TMB) and 1,4-dimethyl-naphthalene (DMN). The reported results show that both s-PS/TMB and s-PS/DMN molecular complexes present intercalate structures and hence s-PS/NB is not a unique case of intercalate complex. In the final part of the paper, by a comparison between several crystal structures and X-ray diffraction literature data, a simple criterion to anticipate the nature (clathrate or intercalate) of s-PS molecular complex phases, just based on the knowledge of their largest Bragg distance, is presented. This analysis also suggests that many other s-PS molecular complexes are expected to present intercalate structures.

2. Experimental section

2.1. Materials

1,3,5-Trimethyl-benzene and 1,4-dimethyl-naphthalene were purchased from Aldrich and used without further purification.

Syndiotactic polystyrene was supplied by Dow Chemical under the trademark Questra 101. ^{13}C nuclear magnetic resonance characterization showed that the content of syndiotactic polystyrene triads was over 98%. The weight-average molar mass obtained by gel permeation chromatography (GPC) in trichlorobenzene at 135 °C was found to be $M_w = 3.2 \times 10^5$ with the polydispersity index, $M_w/M_n = 3.9$.

Uniaxially oriented amorphous films, 20–40 μm thick, have been obtained by monoaxial stretching of the extruded ones, at draw ratio $\lambda \approx 3$, at constant deformation rate of 0.1 s^{-1}, in the temperature range 105–110 °C with a Brukner stretching machine. Uniaxially oriented films, presenting the s-PS/TMB and s-PS/DMN molecular complex phases, have been obtained from oriented amorphous films, by immersion in the pure liquids for 48 h at 50 °C and at room temperature, respectively.

The guest content was determined by thermogravimetric analysis (TGA) and for the samples used for the X-ray diffraction measurements, was in the range 16–20 wt%.

The molecular volume of the guest molecules has been simply evaluated from their molecular mass (M) and density (ρ)

$$V_{guest} = M/\rho N_A$$

where N_A is the Avogadro's number (6.02×10^{23} molecules/mol).

Of course, for small guest molecules (I_2 and CS_2) included in couple into each host cavity, the volume of two molecules has been considered for the plot of Fig. 4.

2.2. X-ray diffraction measurements.

The X-ray fiber diffraction patterns of oriented samples were obtained on a BAS-MS imaging plate (FUJIFILM) with a cylindrical camera (radius 57.3 mm, Ni-filtered Cu Kα radiation monochromatized with a graphite crystal) and processed with a digital scanner (FUJI-BAS 1800).

Calculated structure factors were obtained as $F_{calc} = (\sum |F_i|^2 M_i)^{1/2}$, where M_i is the multiplicity factor and the summation is taken over all reflections included in the 2θ range of the corresponding spot observed in the X-ray fiber diffraction pattern. A thermal factor ($B = 8$ Å^2) and atomic scattering factors from Ref. [9] were used. The observed structure factors F_{obs} were evaluated from the intensities of the reflections observed in the X-ray fiber diffraction pattern (I_{obs})

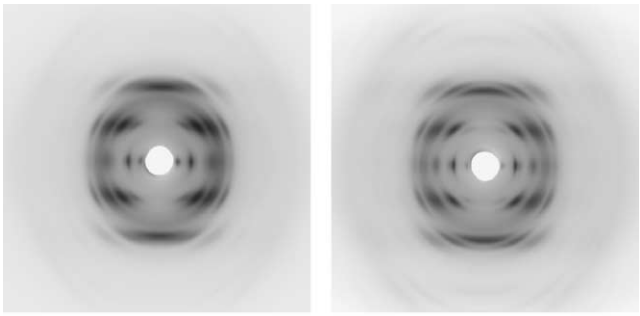

Fig. 1. X-ray fiber diffraction patterns of uniaxially stretched films presenting the s-PS/TMB (A) and the s-PS/DMN (B) molecular complex phases. Fiber axis is vertical.

Table 1
Diffraction angles ($2\theta_{obs}$), Bragg distances (d_{obs}), and intensities (I_{obs}) in arbitrary units (AU) of the reflections observed on the layer lines (l) of the X-ray fiber diffraction pattern of the s-PS/TMB film of Fig. 1A

l	$2\theta_{obs}$ (deg)	d_{obs} (Å)	I_{obs} (AU)
0	5.95	14.85	2519
0	10.20	8.67	5911
0	17.35 (broad)	5.11	8483
0	23.00	3.87	1155
1	14.12	6.27	3062
1	16.67	5.32	10,878
1	19.56	4.54	8521
1	20.66	4.30	
2	23.55	3.78	3107
2	24.77	3.59	3441
2	28.41	3.14	2209
l	34.29	2.62	205

Table 2
Diffraction angles ($2\theta_{obs}$), Bragg distances (d_{obs}), and intensities (I_{obs}) in arbitrary units (AU) of the reflections observed on the layer lines (l) of the X-ray fiber diffraction pattern of the s-PS/DMN film of Fig. 1B

l	$2\theta_{obs}$ (deg)	d_{obs} (Å)	I_{obs} (AU)
0	5.80	15.24	2800
0	10.05	8.80	12,003
0	11.55	7.66	6000
0	15.90 (broad)	5.57	10,528
0	20.00 (broad)	4.44	4476
0	22.60	3.93	3062
1	12.70	6.97	1879
1	15.26	5.81	29,385
1	19.10 (broad)	4.65	29,027
1	23.40	3.80	7906
2	25.07	3.55	9773
2	27.82	3.21	6747
2	30.50	2.93	1062

as $F_{obs}=(I_{obs}/L_p)^{1/2}$, where L_p is the Lorentz-polarization factor for X-ray fiber diffraction

$$L_p = \frac{\left(\frac{0.5(\cos^2 2\theta+\cos^2 2\theta_M)}{1+\cos^2 2\theta_M}+\frac{0.5(1+\cos\ 2\theta_M+\cos^2 2\theta)}{1+\cos\ 2\theta_M}\right)}{(\sin^2 2\theta-\zeta^2)^{1/2}}$$

with $2\theta_M=26.6°$ the inclination angle of the monochromator and $\zeta=\lambda(l/c)$, l and c being the order of the layer line and the chain axis periodicity, respectively, and λ the wavelength of the used radiation (1.5418 Å). The observed intensities I_{obs} were evaluated integrating the crystalline peaks observed in the X-ray diffraction profiles, read along different layer lines, after the subtraction of the amorphous contribution. Owing to the different shapes of the reflections on the equator and on the first and second layer lines, due to the different dimensions of the lamellar crystals in the direction perpendicular and parallel to the chain axis, different factors have been used to scale the observed and calculated structure factors on the diverse layer lines. The discrepancy factor R has been evaluated as $R=\sum|F_{obs}-F_{calc}|/\sum F_{obs}$ taking into account only the observed reflections.

2.3. Calculation methods

Energy calculations were carried out by using commercially available software (*Cerius*^{2} version 4.2 by Accelrys, Inc.). The force field used was the compass force field [10]. Energy was minimized using the open force field module by smart minimizer method with standard convergence. The

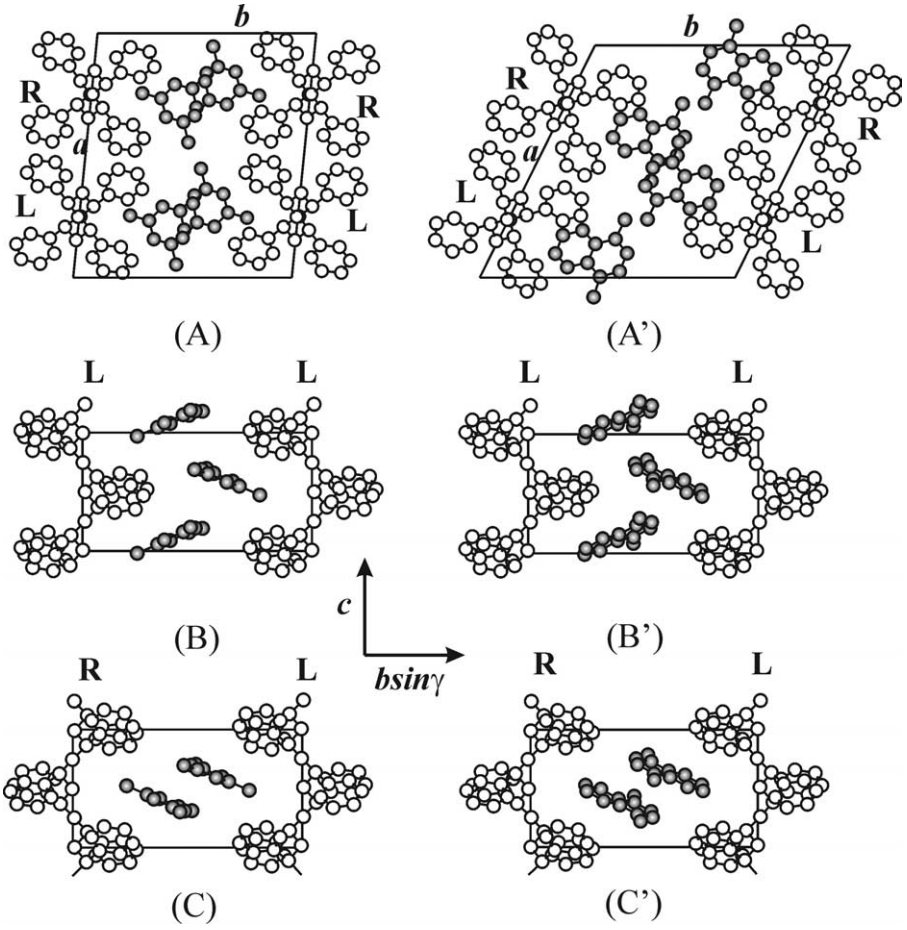

Fig. 2. Packing model proposed for the crystal structures of s-PS molecular complex containing 1,3,5-trimethyl-benzene (A, B, C) and 1,4-dimethyl-naphthalene(A′, B′, C′), in the space group $P2_1/a$. In (A, A′) the whole content of the unit cell in the *ab* projection is shown while in (B, B′) and (C, C′) the *cbsinγ* projections of the packing between only one couple of isomorphous (along *b* direction) and only one couple of enantiomorphous (along $b+a/2$ direction) polymer chains, are shown respectively. R, right-handed; L, left-handed helices.

starting conformation of the s-PS polymer chains corresponds to that found by molecular mechanics calculations reported in literature [11]. Since the value of the *a* axis of the unit cell is almost identical to those found for all the clathrate structures of this polymer described so far, all the starting models were characterized by an orientation of the polymer chains along the *a* axis direction similar to that found for those clathrates, while the independent guest molecule was placed in the space between the *ac* layers of chains by trial procedure.

3. Results

3.1. X-ray diffraction data

The X-ray fiber diffraction pattern of a uniaxially oriented film presenting the s-PS/TMB molecular complex phase is reported in Fig. 1A while that one of the s-PS/DMN molecular complex is reported in Fig. 1B. All the reflections observed in the fiber diffraction patterns of Fig. 1A and B are listed in Tables 1 and 2, respectively.

3.2. Determination of the crystal structures

3.2.1. 1,3,5-Trimethyl-benzene

The reflections shown in Fig. 1A and listed in Table 1 can be indexed in terms of a monoclinic cell with constants $a=17.3$ Å, $b=15.4$ Å, $c=7.8$ Å and $\gamma=95.7°$. The space

Table 3
Fractional coordinates of the atoms of an asymmetric unit of the model proposed (Fig. 2A–C) for the molecular complex of s-PS with 1,3,5-trimethyl-benzene

	x/a	*y/b*	*z/c*
C1	0.154	0.004	0.245
C2	0.195	−0.056	0.365
C3	0.251	−0.005	0.492
C4	0.292	−0.061	0.623
C5	0.133	−0.114	0.462
C6	0.083	−0.080	0.579
C7	0.028	−0.134	0.669
C8	0.021	−0.224	0.642
C9	0.070	−0.259	0.525
C10	0.125	−0.204	0.437
C11	0.339	−0.125	0.530
C12	0.401	−0.097	0.422
C13	0.443	−0.157	0.339
C14	0.424	−0.246	0.363
C15	0.362	−0.275	0.471
C16	0.320	−0.214	0.552
C17	−0.234	−0.678	0.057
C18	−0.157	−0.649	0.095
C19	−0.137	−0.567	0.165
C20	−0.196	−0.514	0.196
C21	−0.274	−0.541	0.160
C22	−0.291	−0.625	0.090
C23	−0.337	−0.483	0.194
C24	−0.255	−0.768	−0.019
C25	−0.054	−0.535	0.204

Hydrogen atoms were included in the structure factors calculation, but they are omitted in this table for simplicity.

Table 4
Comparison between calculated (F_{calc}) and observed structure factors (F_{obs}), evaluated from the intensities observed in the X-ray fiber diffraction pattern of Fig. 1A, for the model of the molecular complex of s-PS with 1,3,5-trimethyl-benzene of Fig. 2(A–C)

hkl	d_{obs} (Å)	d_{calc} (Å)	F_{calc}		F_{obs}
0 1 0	14.85	15.32	56		53
2 0 0	8.67	8.61	103		107
0 2 0	–	7.66	33		–
$\bar{2}$ 2 0		6.03	38		
2 2 0		5.46	97		
0 3 0		5.11	56		
$\bar{2}$ 3 0	5.11	4.60	105		
4 0 0		4.30	17	167	169
$\bar{4}$ 1 0		4.26	38		
2 3 0		4.21	19		
4 1 0		4.04	23		
$\bar{4}$ 2 0		3.92	13		
0 4 0	3.87	3.83	75	77	72
2 4 0	–	3.38	47		–
$\bar{2}$ 5 0	–	2.98	39		–
6 1 0	–	2.77	37		–
$\bar{6}$ 4 0	–	2.41	50		–
4 5 0	–	2.39	36		–
0 1 1	–	6.95	32		–
$\bar{1}$ 1 1		6.55	16		
1 1 1	6.27	6.35	59	62	82
2 0 1		5.78	21		
$\bar{2}$ 1 1		5.53	46		
0 2 1	5.32	5.47	49		
$\bar{1}$ 2 1		5.32	128	189	188
2 1 1		5.29	32		
1 2 1		5.11	116		
$\bar{2}$ 2 1		4.77	7		
3 0 1		4.62	49		
$\bar{3}$ 1 1		4.53	113		
2 2 1	4.54	4.47	50		
3 1 1		4.33	122		
0 3 1		4.27	51	201	191
$\bar{1}$ 3 1	4.30	4.23	18		
3 2 1		4.11	64		
1 3 1		4.07	1		
$\bar{2}$ 3 1		3.96	27		
3 2 1		3.82	14		
4 0 1		3.77	117		
$\bar{4}$ 1 1	3.78	3.74	71		
2 3 1		3.71	15	142	132
4 1 1		3.59	4		
$\bar{3}$ 3 1		3.57	35		
$\bar{4}$ 2 1	–	3.50	36		–
5 1 1	–	3.03	37		–
1 5 1	–	2.77	33		–
2 5 1	–	2.64	30		–
1 1 2		3.67	27		145
2 0 2		3.55	57		
$\bar{2}$ 1 2		3.49	23		
$\bar{1}$ 2 2	3.59	3.48	104	145	
0 2 2		3.44	18		
2 1 2		3.43	27		
1 2 2		3.38	68		

(continued on next page)

Table 4 (*continued*)

hkl	d_{obs} (Å)	d_{calc} (Å)	F_{calc}		F_{obs}
$\bar{2}$ 2 2		3.27	23		
3 0 2		3.23	18		
$\bar{3}$ 1 2		3.19	49		
2 2 2		3.17	47		
3 1 2		3.12	80		
0 3 2		3.10	49		
$\bar{1}$ 3 2	3.14	3.08	19	149	161
$\bar{3}$ 2 2		3.03	62		
1 3 2		3.02	18		
$\bar{2}$ 3 2		2.97	8		
3 2 2		2.92	8		
4 0 2		2.89	25		
$\bar{4}$ 1 2		2.88	46		
2 3 2		2.86	20		
1 4 2		2.67	4		
3 3 2		2.66	11		
$\bar{2}$ 4 2		2.66	8		
4 2 2	2.62	2.65	37		
$\bar{4}$ 3 2		2.59	54	74	62
5 0 2		2.58	24		
$\bar{5}$ 1 2		2.58	9		
2 4 2		2.55	20		

The Bragg distances (d_{obs}), observed in the X-ray fiber diffraction pattern and calculated (d_{calc}) for the proposed monoclinic unit cell ($a=17.3$ Å, $b=15.4$ Å, $c=7.8$ Å and $\gamma=95.7°$), are also shown. Reflections not observed with F_{calc} less than 30 have not been reported. F_{obs} reported have been scaled by a factor 3.7 on the equatorial layer line, 4.4 on the first layer line and 7.1 on the second layer line.

Table 5
Fractional coordinates of the atoms of an asymmetric unit of the model proposed (Fig. 2(A′, B′, C′)) for the molecular complex of s-PS with DMN. Hydrogen atoms were included in the structure factors calculation, but they are omitted in this table for simplicity

	x/a	*y/b*	*z/c*
C1	0.158	0.007	0.246
C2	0.175	−0.054	0.366
C3	0.250	−0.005	0.492
C4	0.269	−0.062	0.622
C5	0.094	−0.109	0.464
C6	0.058	−0.072	0.579
C7	−0.017	−0.122	0.668
C8	−0.059	−0.212	0.641
C9	−0.025	−0.250	0.524
C10	0.051	−0.198	0.438
C11	0.294	−0.125	0.531
C12	0.365	−0.098	0.424
C13	0.388	−0.157	0.344
C14	0.339	−0.246	0.371
C15	0.267	−0.275	0.477
C16	0.245	−0.215	0.555
C17	−0.436	0.606	0.647
C18	−0.496	0.530	0.727
C19	−0.355	0.613	0.594
C20	−0.334	0.543	0.623
C21	−0.297	0.689	0.509
C22	−0.318	0.756	0.475
C23	−0.396	0.751	0.527
C24	−0.455	0.677	0.612
C25	−0.395	0.470	0.702
C26	−0.474	0.464	0.753
C27	−0.584	0.516	0.786
C28	−0.251	0.544	0.570

Table 6
Comparison between calculated (F_{calc}) and observed structure factors (F_{obs}), evaluated from the intensities observed in the X-ray fiber diffraction pattern of Fig. 1B, for the model of the molecular complex of s-PS with 1,4-dimethylnaphthalene of Fig. 2(A′, B′, C′)

hkl	d_{obs} (Å)	d_{calc} (Å)	F_{calc}		F_{obs}
0 1 0	15.24	15.39	21		37
$\bar{2}$ 1 0	8.80	8.70	93		101
2 0 0		7.81	18		
0 2 0	7.66	7.69	42	62	76
$\bar{2}$ 2 0		7.36	42		
2 1 0		5.97	39		
$\bar{2}$ 3 0	5.57	5.57	89	116	119
0 3 0		5.13	64		
2 2 0		4.56	52		
$\bar{4}$ 2 0		4.35	41		
$\bar{2}$ 4 0	4.44	4.29	74	100	88
$\bar{4}$ 1 0		4.26	13		
4 0 0		3.91	33		
0 4 0	3.93	3.85	101	106	77
2 3 0	–	3.61	56		–
$\bar{2}$ 5 0	–	3.43	21		–
0 5 0	–	3.08	33		–
$\bar{2}$ 6 0	–	2.84	35		–
$\bar{6}$ 4 0	–	2.81	26		–
$\bar{6}$ 1 0	–	2.78	21		–
6 0 0	–	2.60	33		–
0 6 0	–	2.56	35		–
$\bar{6}$ 6 0	–	2.45	33		–
$\bar{4}$ 7 0	–	2.43	41		–
4 4 0	–	2.28	41		–
1 0 1		6.98	11		
0 1 1	6.97	6.96	31	53	34
$\bar{1}$ 1 1		6.89	41		
1 1 1		5.93	77		
$\bar{2}$ 1 1		5.81	28		
$\bar{1}$ 2 1		5.77	115		
2 0 1	5.81	5.52	29	149	185
0 2 1		5.48	34		
$\bar{2}$ 2 1		5.35	17		
2 1 1		4.74	81		
1 2 1		4.72	116		
$\bar{3}$ 1 1		4.64	50		
$\bar{1}$ 3 1		4.59	55		
$\bar{3}$ 2 1	4.65	4.56	86	243	228
$\bar{2}$ 3 1		4.53	26		
3 0 1		4.33	128		
0 3 1		4.29	35		
$\bar{3}$ 3 1		4.15	90		
3 1 1		3.82	25		
$\bar{4}$ 2 1		3.80	91		
1 3 1		3.79	9		
$\bar{2}$ 4 1	3.80	3.76	9	140	138
$\bar{4}$ 1 1		3.74	64		
$\bar{1}$ 4 1		3.69	30		
$\bar{4}$ 3 1		3.64	69		
$\bar{3}$ 4 1		3.62	28		

(continued on next page)

Table 6 (*continued*)

hkl	d_{obs} (Å)	d_{calc} (Å)	F_{calc}		F_{obs}
1 4 1	–	3.12	39		–
2 4 1	–	2.77	43		–
$\bar{6}$ 2 1	–	2.71	38		–
$\bar{5}$ 6 1	–	2.50	38		–
1 1 2		3.59	39		
$\bar{2}$ 1 2		3.56	9		
$\bar{1}$ 2 2		3.55	51		
2 0 2	3.55	3.49	102	172	168
0 2 2		3.48	119		
$\bar{2}$ 2 2		3.45	30		
2 1 2		3.27	91		
1 2 2		3.26	78		
$\bar{3}$ 1 2		3.23	20		
$\bar{1}$ 3 2		3.21	1		
$\bar{3}$ 2 2	3.21	3.21	50	188	179
$\bar{2}$ 3 2		3.20	32		
3 0 2		3.12	99		
0 3 2		3.10	43		
$\bar{3}$ 3 2		3.05	80		
2 2 2		2.96	29		
3 1 2		2.91	6		
$\bar{4}$ 2 2		2.90	53		
1 3 2	2.93	2.90	28	68	81
$\bar{2}$ 4 2		2.89	9		
$\bar{4}$ 1 2		2.88	6		
4 0 2	–	2.76	44		–
$\bar{4}$ 4 2	–	2.68	65		–

The Bragg distances (d_{obs}), observed in the X-ray fiber diffraction pattern and calculated (d_{calc}) for the proposed monoclinic unit cell ($a=17.44$ Å, $b=17.18$ Å, $c=7.8$ Å and $\gamma=116.4°$), are also shown. Reflections not observed with F_{calc} less than 20 have not been reported. F_{obs} reported have been scaled by a factor 2.5 on the equatorial layer line, 2.9 on the first layer line and 4.7 on the second layer line.

group is $P2_1/a$, in agreement with the systematic absence of *hk0* reflections with $h=2n+1$ and *00l* reflections with $l=2n+1$.

The volume of the proposed unit cell is appropriate for a molar ratio 2 between monomeric units and guest molecule, corresponding to a calculated (1.05 g/cm^3) density not far from the experimental density value observed for these semicrystalline films, as well as for amorphous s-PS films.

Consequently, packing energy calculations have been performed according to the space group $P2_1/a$ considering an asymmetric unit made of two monomeric units of s-PS and one guest molecule, keeping the axes of the unit cell constant. The best result was found for the situation represented in Fig. 2(A–C). The discrepancy factor *R* for this model is 6%.

The fractional coordinates of an asymmetric unit of the proposed model are listed in Table 3. Table 4 compares the calculated and the observed structure factors.

3.2.2. 1,4-Dimethyl-naphthalene

The reflections shown in Fig. 1B and reported in Table 2 can be indexed in terms of a monoclinic cell with constants

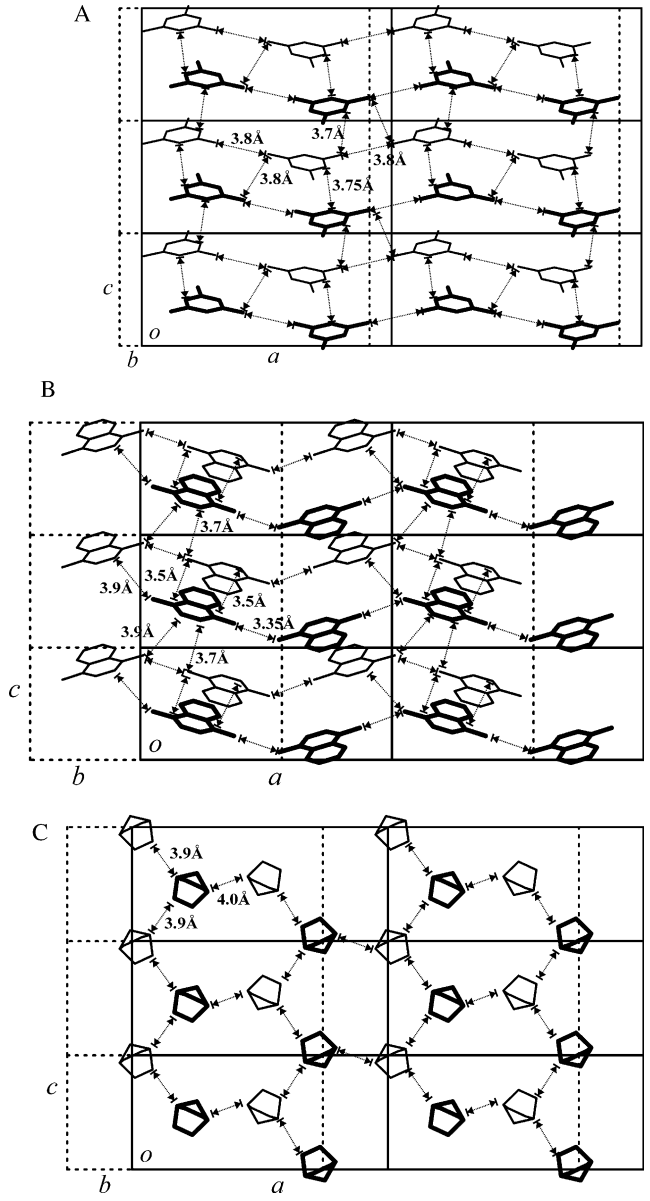

Fig. 3. Projection perpendicular to the *ac* plane of layers of guest molecules parallel to the *ac* polymer layers: 1,3,5-trimethyl-benzene (A), 1,4-dimethyl-naphthalene (B) and bicyclo[2,2,1]-hepta-2,5-diene (C). Six unit cells are shown. Guest molecules near to the reader are represented with bold lines. The shortest distances between neighboring guest molecules are also indicated.

$a=17.4$ Å, $b=17.2$ Å, $c=7.8$ Å and $\gamma=116.4°$. The space group is $P2_1/a$, in agreement with the systematic absence of *hk0* reflections with $h=2n+1$ and *00l* reflections with $l=2n+1$. Also in this case, the volume of the proposed unit cell is appropriate for the molar ratio 2 between monomeric units and guest molecule, corresponding to a calculated (1.16 g/cm^3) density not far from the experimental density value ($\approx$1.07 g/cm^3).

Packing energy calculations have been performed according the space group $P2_1/a$ considering an asymmetric unit made of two monomeric units of s-PS and one guest molecule, keeping the axes of the unit cell constant. The best result was found for

the situation represented in Fig. 2(A′, B′, C′). The discrepancy factor *R* for this model is 12%.

The fractional coordinates of an asymmetric unit of the proposed model are listed in Table 5. Table 6 compares the calculated and the observed structure factors.

3.3. Packing analysis

In the case of the s-PS/TMB complex, the shortest distances between non-bonded atoms are those typical of the crystal structures of hydrocarbons (in fact, all distances between guest molecules and polymer chains and all guest-guest contact distances in the final packing model are greater than 3.7 Å, while all the distances among atoms belonging to different chains are greater than 3.9 Å). For what concern the s-PS/DMN complex, we found some slightly shorter distances. In particular, some distances between carbon atoms equal to 3.46 Å characterize couples of 1,4-dimethyl-naphthalene molecules related by a center of inversion. These distances can be justified taking into account the fact that the hydrogen atoms bonded to sp2 carbon are coplanar to the plane of the molecule itself. All the other distances are greater than 3.7 Å with the exception of a distance between methyl groups belonging to different guest molecules of 3.35 Å, that is likely to be tolerated to allow the efficient approach between 1,4-dimethyl-naphthalene molecules described before (see Fig. 3B for more details).

4. Discussion

4.1. Two new s-PS intercalate molecular complexes

The packing models proposed for the s-PS molecular complexes with TMB and DMN present guest molecules arranged in layers, each guest molecule being placed at van der Waals distance from at least other three neighboring guest molecules, thus leading to guest/monomeric-unit molar ratios equal to 1/2. These features also characterize the s-PS/NB molecular complex, i.e. the first and only s-PS molecular complex with known intercalate crystalline structure [2h]. The similarity between the three intercalate s-PS structures is clearly shown in Fig. 3, comparing guest layers alternated and parallel to the polymer *ac* layer, for s-PS/TMB (3A), s-PS/DMN (3B) and s-PS/NB (3C) [2h] intercalates.

It is worth noting that the two new intercalate structures presented in this paper are characterized by the same packing of enantiomorphous helices along the *ac* layers already found for the intercalate structure with NB [2h], for all clathrate forms [2a–g] and for δ form [3a] of s-PS. In fact, the *a* axis for all these crystalline forms is very similar, only varying in the range 17.35 ± 0.25 Å. This clearly indicates that the formation of the molecular complex phases of s-PS is dominated by the formation of mono-layers of efficiently packed enantiomorphous s(2/1)2 helices.

4.2. Intercalate versus clathrate molecular complexes

As discussed above, the mono-layer of enantiomorphous s(2/1)2 polymer helices, parallel to the *ac* crystalline planes, is a structural feature which is common to the δ phase of s-PS as well as to all clathrate and intercalate molecular complexes. As a consequence, particularly informative can be the comparison between the spacing of the Bragg planes 010 (d_{010}) for all molecular complex crystalline phases of s-PS, with known crystal structures (upper part of Table 7) [2,3]. This spacing corresponds to the maximum Bragg distance (d_{max}), associated with the crystalline peak at lowest diffraction angle. For molecular complex phases with unknown crystal structures, observed for semicrystalline s-PS samples [12] or only for physical gels [13] (middle and bottom part of Table 7, respectively), we can make the hypothesis that the d_{max} values can also correspond to the spacing of the Bragg planes 010 (d_{010}).

For all molecular complex phases of Table 7, the d_{max} distance has been plotted versus the molecular volume of the guest (second column) in Fig. 4. It is apparent that, for the well-established clathrate phases (filled squares) as well as for most molecular complexes (empty squares), as the volume of the guest molecules increases up to 120–160 Å^3 (i.e. the estimated volume of the cavity of the δ phase) [3b], the d_{max} value remains close to that one of the empty δ phase (10.5 Å), while as the volume of the guest molecules further increases, a progressive small increase of the d_{max} value up to nearly 12 Å is observed. This analysis clearly suggests that molecular complexes indicated by empty squares are expected to have a clathrate structure.

On the other hand, for the three well-established intercalate phases (filled circles) and for molecular complex phases with anthracene and 3-carene (3,7,7-trimethylbicyclo[4.1.0]hept-3-ene), observed in semicrystalline samples (empty circles), and with benzene, benzylmethacrylate, cyclohexylmethacrylate, only observed in physical gels (crossed circles), the experimental points are well above the generally observed behavior. This analysis clearly suggests that molecular complexes indicated by empty and crossed circles are expected to have an intercalate structure.

More in general, as a simple criterion, we suggest that clathrate and intercalate structures can be anticipated for s-PS molecular complexes with $d_{max} < 12$ Å and $d_{max} > 13$ Å, respectively.

Further studies are in progress aimed to establish the guest requirements suitable to get clathrate or intercalate s-PS molecular complex phases.

5. Conclusion

The crystalline structures of molecular complexes of syndiotactic polystyrene with 1,3,5-trimethyl-benzene and 1,4-dimethyl-naphthalene have been described. In both cases, the s(2/1)2 polymer helices and guest molecules are packed according to the space group $P2_1/a$. The unit cell constants are: $a = 17.3$ Å, $b = 15.4$ Å, $c = 7.8$ Å and $\gamma = 95.7°$ for s-PS/TMB

Table 7
Comparison between the molecular complex crystalline phases of s-PS with different guests

Guest	Guest volume (Å)^3	2θ Cu Kα (deg.)	d_{max} (Å)	References	Notes
s-PS δ form	120–160[a]	8.4	10.5	[3a]	$d_{max}=d_{010}$
1,2-Dichloroethane	131	8.4	10.5	[2e]	Known crystalline structures (clathrates) $d_{max}=d_{010}$
Carbon disulfide	200	8.3	10.6	[2f]	
o-Dichlorobenzene	187	7.95	11.1	[2g]	
Iodine	171	7.97[b]	11.1	[2d]	
Toluene	177	7.9	11.2	[2c,3a]	
Norbornadiene	169	6.6	13.4	[2h]	Known crystalline structures (intercalates) $d_{max}=d_{010}$
1,3,5-Trimethylbenzene	230	5.95	14.85	This work	
1,4-Dimethylnaphthalene	255	5.8	15.2	This work	
Chloropropane	146	8.35	10.6	[12a]	Molecular complexes with unknown crystalline structures
Trichloroethylene	149	8.3	10.6	[7b]	
Methylene chloride	106	8.2	10.8	[2a,12b]	
1,2-Dichloropropane	158	8.2	10.8	[12a]	
Chloroform	133	8.1	10.9	[4a]	
Heptane	243	8.0	11.05	[12c]	
Decane	323	8.0	11.05	[12d]	
Tetrahydrofuran	135	8.0	11.05	[7c]	
p-Chlorotoluene	196	7.95	11.2	[12e]	
p-Xylene	204	7.9	11.2	[4e]	
Styrene	190	7.9	11.2	[12f]	
1,2,4-Trichlorobenzene	207	7.9	11.2	Our data	
p-Chlorostyrene	199	7.9	11.2	[12g]	
o-Xylene	203	7.87	11.2	[12h]	
Hexane	217	7.82	11.3	[12c,d]	
Benzene	148	7.82	11.3	[7c]	
p-Cresol	174	7.85	11.3	[12j]	
Ethylbenzene	116	7.73	11.4	[12i]	
Naphthalene	208	7.7	11.5	[8a]	
Cyclohexane	179	7.6	11.6	Our data	
m-Xylene	203	7.6	11.6	[4e]	
Indene	194	7.6	11.6	Our data	
p-Methylstyrene	219	7.6	11.6	Our data	
Decaline (*cis*/*trans*)	265	7.4	11.9	Our data	
3-Carene	264	6.2	14.3	Our data	
Anthracene	231	5.05	17.5	[12j]	
Cycloexylmethacrylate	290	6.0	14.7	[13c]	Molecular complex phases in gels
Benzene	148	5.95	14.85	[13a]	
Benzylmethacrylate	281	5.8	15.2	[13b]	

The guest volume, the observed lowest diffraction angle (2θ, for Cu Kα radiation) and the corresponding Bragg distance (d_{max}) are reported.
[a] Estimated volume of the crystalline cavities of the s-PS δ form [3b].
[b] For the s-PS/iodine molecular complex, rather than the experimental value (not available), the $2\theta_{010}$ calculated from the unit cell parameters reported in Ref. [2d] has been indicated.

complex and $a=17.4$ Å, $b=17.2$ Å, $c=7.8$ Å and $\gamma=116.4°$ for s-PS/DMN complex.

As for all s-PS molecular complexes [2], layers of polymer chains, with a very efficient close packing of enantiomorphous s(2/1)2 helices, are present in the *ac* planes. In fact, for all the s-PS molecular complexes the *a* axis remains practically independent of the chemical nature of the guest molecule and close to that one observed for the nanoporous δ phase.

These *ac* layers of polymer helices, for both s-PS/TMB and s-PS/DMNP structures, are alternated with layers of contiguous guest molecules, thus leading to a guest/-monomeric-unit molar ratio of 1/2. These structural features, also common to the already known structure of the s-PS molecular complex with norbornadiene, indicate both new molecular complexes as intercalates. Most known s-PS molecular complexes can be instead defined as clathrates since a closer packing between the *ac* polymer layers produce isolation of the guest molecules (into the cavities typical of the nanoporous δ phase), thus leading to a typical guest/monomeric-unit molar ratio of 1/4.

A comparison between crystalline structures and X-ray diffraction patterns of several s-PS molecular complex phases, being present in semicrystalline samples or in physical gels, has suggested a simple criterion to anticipate the intercalate or clathrate nature of s-PS molecular complexes. In particular, clathrate and intercalate structures are expected for molecular

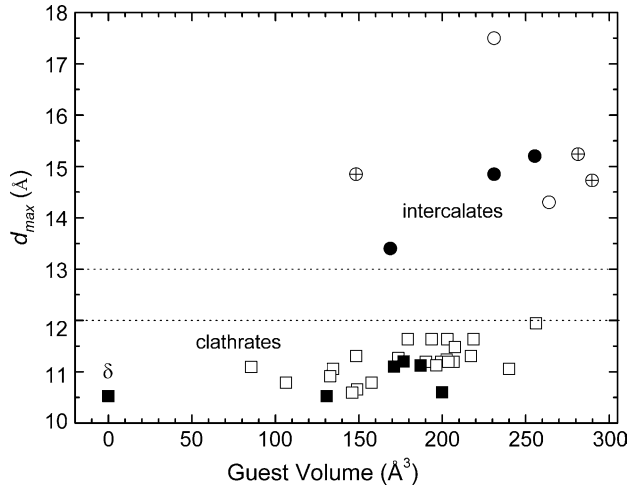

Fig. 4. Maximum Bragg distance (d_{max}) for several s-PS molecular complex crystalline phases with different guests versus the guest molecular volume. Squares indicate clathrates while circles indicate intercalates. s-PS molecular complexes with unknown crystal structures are indicated with empty symbols while crossed circles indicate crystalline phases in s-PS physical gels. For molecular complexes with established clathrate (full squares) and intercalate (full circles) crystal structures, d_{max} is equal to the distance between *ac* layers of helices (d_{010}). The plot suggests that molecular complexes with $d_{max} < 12$ Å and $d_{max} > 13$ Å, are expected to present clathrate and intercalate structures, respectively.

complexes with $d_{max} < 12$ Å and $d_{max} > 13$ Å (d_{max} being their maximum Bragg distance), respectively.

Acknowledgements

Financial support of the 'Ministero dell'Istruzione, dell'Università e della Ricerca' (PRIN2004 and FIRB2001); and of 'Regione Campania' (Legge 5 and Centro di Competenza per le Attività Produttive) is gratefully acknowledged. We thank Dr Christophe Daniel of University of Salerno for useful discussions.

References

[1] (a) Guerra G, Vitagliano MV, De Rosa C, Petraccone V, Corradini P. Macromolecules 1990;23:1539–44.
(b) Chatani Y, Stimane Y, Inoue Y, Inagaki T, Ishioka T, Iijtsu T, Yukimori T. Polymer 1992;33:488–92.
[2] (a) Immirzi A, de Candia F, Iannelli P, Zambelli Z, Vittoria V. Macromol Chem Rapid Commun 1988;9:761–4.
(b) Vittoria V, de Candia F, Iannelli P, Immirzi A. Makromol Chem, Rapid Commun 1988;9:765–9.
(c) Chatani Y, Shimane Y, Inagaki T, Iijtsu T, Yukimori T, Shikuma H. Polymer 1993;34:1620–4.
(d) Chatani Y, Inagaki T, Shimane Y, Shikuma H. Polymer 1993;34:4841–5.
(e) De Rosa C, Rizzo P, Ruiz de Ballesteros O, Petraccone V, Guerra G. Polymer 1999;40:2103–10.
(f) Tarallo O, Petraccone V. Macromol Chem Phys 2004;205:1351–60.
(g) Tarallo O, Petraccone V. Macromol Chem Phys 2005;206:672–9.
(h) Petraccone V, Tarallo O, Venditto V, Guerra G. Macromolecules 2005;38:6965–71.
[3] (a) De Rosa C, Guerra G, Petraccone V, Pirozzi B. Macromolecules 1997;30:4147–52.
(b) Milano G, Venditto V, Guerra G, Cavallo L, Ciambelli P, Sannino D. Chem Mater 2001;13:1506–11.
[4] (a) Manfredi C, Del Nobile MA, Mensitieri G, Guerra G, Rapacciuolo M. J Polym Sci, Polym Phys Ed 1997;35:133–40.
(b) Guerra G, Milano G, Venditto V, Musto P, De Rosa C, Cavallo L. Chem Mater 2000;12:363–8.
(c) Musto P, Mensitieri G, Cotugno S, Guerra G, Venditto V. Macromolecules 2002;35:2296–304.
(d) Sivakumar M, Yamamoto Y, Amutharani D, Tsujita Y, Yoshimizu H, Kinoshita T. Macromol Rapid Commun 2002;23:77–9.
(e) Yamamoto Y, Kishi M, Amutharani D, Sivakumar M, Tsujita Y, Yoshimizu H. Polym J 2003;35:465–9.
(f) Daniel C, Alfano D, Venditto V, Cardea S, Reverchon E, Larobina D, et al. Adv Mater 2005;17:1515–8.
[5] (a) Mensitieri G, Venditto V, Guerra G. Sensors Actuat B 2003;92:255–61.
(b) Giordano M, Russo M, Cusano A, Cutolo A, Mensitieri G, Nicolais L. Appl Phys Lett 2004;85:5349–51.
(c) Giordano M, Russo M, Cusano A, Mensitieri G, Guerra G. Sensors Actuat B 2005;109:177–84.
(d) Arpaia P, Guerra G, Mensitieri G, Schiano Lo Moriello R. IEEE Trans Instrum Meas 2005;54:31–7.
[6] (a) Albunia AR, Di Masi S, Rizzo P, Milano G, Musto P, Guerra G. Macromolecules 2003;36:8695.
(b) Albunia AR, Milano G, Venditto V, Guerra G. J Am Chem Soc 2005;127:13114–5.
[7] (a) Rizzo P, Lamberti M, Albunia A, Ruiz de Ballesteros O, Guerra G. Macromolecules 2002;35:5854–960.
(b) Rizzo P, Costabile A, Guerra G. Macromolecules 2004;37:3071–6.
(c) Rizzo P, Della Guardia S, Guerra G. Macromolecules 2004;37:8043–9.
(d) Rizzo P, Spatola A, De Girolamo Del Mauro A, Guerra G. Macromolecules. 2005;38:10089–94.
[8] (a) Venditto V, Milano G, De Girolamo Del Mauro A, Guerra G, Mochizuki J, Itagaki H. Macromolecules 2005;38:3696–702.
(b) Stegmaier P, De Girolamo Del Mauro A, Venditto V, Guerra G. Adv Mater 2005;17:1166–8.
(c) Uda Y, Kaneko F, Tanigaki N, Kawaguchi T. Adv Mater 2005;17:1846–50.
[9] Cromer DT, Mann JB. Acta Crystallogr 1968;A24:321–4.
[10] Sun H. J Phys Chem B 1998;102:7338–64.
[11] Corradini P, Napolitano R, Pirozzi B. Eur Polym J 1990;26:157–61.
[12] (a) Musto P, Manzari M, Guerra G. Macromolecules 2000;33:143–9.
(b) Bhoje Gowd E, Nair SS, Ramesh C. Macromolecules 2002;35:8509–14.
(c) Guerra G, Milano G, Venditto V, Loffredo F, Ruiz de Ballesteros O, Cavallo L, De Rosa C. Makromol Chem Phys, Makromol Symp 1999;138:131–7.
(d) Uda Y, Kaneko F, Kawaguchi T. Macromol Rapid Commun 2004;25:1900–4.
(e) Mahesh KPO, Sivakumar M, Yamamoto Y, Tsujita Y, Yoshimizu H, Okamoto S. J Polym Sci, Polym Phys 2004;42:3439–46.
(f) Reverchon E, Guerra G, Venditto V. J Appl Polym Sci 1999;74:2077–82.
(g) De Girolamo Del Mauro A, Loffredo F, Venditto V, Longo P, Guerra G. Macromolecules 2003;36:7577–84.
(h) Loffredo F, Pranzo A, Venditto V, Longo P. Macromol Chem Phys 2003;204:859–67.
(i) Sivakumar M, Mahesh KPO, Yamamoto Y, Yoshimizu H, Tsujita Y. J Polym Sci, Polym Phys 2005;43:1873–80.
(j) Tsujita Y, Yoshimizu H, Okamoto S. J Mol Struct 2005;739:3–12.
[13] (a) Daniel C, Deluca MD, Guenet JM, Brulet A, Menelle A. Polymer 1996;37:1273–80.
(b) Rastogi S, Goossens JGP, Lemstra PJ. Macromolecules 1998;31:2983–98.
(c) van Hooy-Corstjens CSJ, Magusin PCMM, Rastogi S, Lemstra PJ. Macromolecules 2002;35:6630–7.